

Study of the 1D Scattering Mechanisms' Impact on the Mobility in Si Nanowire Transistors

C. Medina-Bailon^{*†}, T. Sadi[‡], M. Nedjalkov[§], J. Lee[†], S. Berrada[†], H. Carrillo-Nunez[†], V. Georgiev[†], S. Selberherr[§], and A. Asenov[†]

[†] School of Engineering, University of Glasgow, Glasgow G12 8LT, Scotland, UK

[‡] Department of Neuroscience and Biomedical Engineering, Aalto University, P.O. Box 12200, FI-00076 Aalto, Finland

[§] Institute for Microelectronics, TU-Wien, Gußhausstraße 27-29/E360, A-1040 Vienna, Austria

* e-mail: Cristina.MedinaBailon@glasgow.ac.uk

Abstract—The extensive research of aggressively scaled nano-electronic devices necessitates the inclusion of quantum confinement effects and their impact on performance. This work implements a set of multisubband phonon and impurity scattering mechanisms within the Kubo-Greenwood formalism in order to study their impact on the mobility in Si nanowire transistors (NWTs). This 1D treatment has been coupled with a 3D Poisson-2D Schrödinger solver, which accurately captures the effects of quantum confinement on charge dynamics. We also emphasize the importance of using the 1D models to evaluate the geometrical properties on mobility at the scaling limit.

Index Terms—Phonon Scattering; Impurity Scattering; Kubo-Greenwood Formalism; Matthiessen rule; Nanowire FETs

I. INTRODUCTION

Nanowire transistors (NWTs) are being considered as potential candidates for replacing FinFETs in aggressively scaled CMOS technology due to their better electrostatic integrity. NWTs are suitable for CMOS scaling beyond the 5nm node [1]. In the corresponding simulation technologies, the reduction of the characteristic confined dimensions increases the importance of including quantum mechanical effects. Accordingly, it has been mandatory to develop different schemes in order to reduce the computational effort of these quantum transport simulations. One of the most popular approaches is to incorporate the quantum effects into semi-classical simulation models with refined macroscopic quantities. The low-field electron mobility is one of the parameters which determines the NWTs performance [2]. Therefore, its study using novel computational techniques remains of continuing interest.

The approach considered herein combines quantum effects with the semi-classical Boltzmann transport equation (BTE) within the relaxation time approximation of a 1D electron gas adopting the Kubo-Greenwood formalism [3]–[5]. This strategy delivers reliable mobility values at low-field near-equilibrium conditions, based on the rates of the relevant scattering mechanisms governing the multisubband transport in NWTs [6]. The cumulative effect of the scattering probabilities is then calculated by applying the Matthiessen rule [7]. This combined semi-classical strategy allows the computation of each mechanism separately due to the probability based Matthiessen rule. In contrast, purely quantum transport theory involves phases and amplitudes and so it precludes a separate treatment of the involved physical phenomena. In this work,

we study the effects of quantum confinement on the electron mobility in NWTs including phonon and impurity scatterings. In addition, we analyze the impact of the nanowire size and geometry on the transport properties.

II. METHODOLOGY

Long-channel device simulations provide a convenient framework for assessing low-field electron mobilities in the presence of strong confinement effects in devices such as NWTs. We directly study the effects of charge confinement on transport as a function of out-of-plane (lateral) applied low electric field. In the chosen framework, we pre-calculate the potential profile and the corresponding eigenvalues and eigenfunctions of the subbands in the NWT cross section.

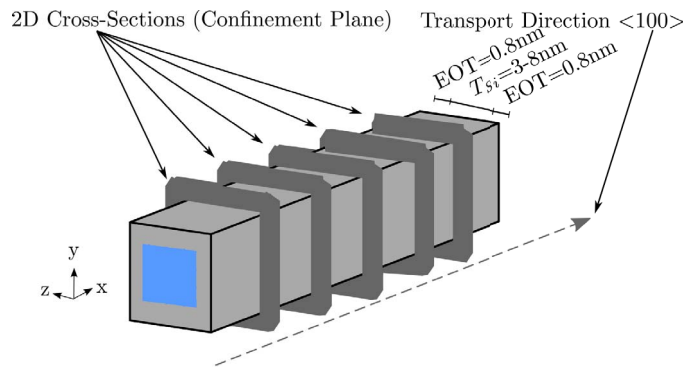


Fig. 1. NWT structures analyzed in this work with widths ranging from 3nm to 8nm. The coupled 2D Schrödinger and 3D Poisson equation are solved for each cross-section (confinement plane) and then the scattering rates are calculated accounting for the potential and the eigenfunctions for each subband.

For calculating the mobilities with the aforementioned assumption, some steps are needed in the simulation scheme. First, the channel is assumed to be infinitely long and the electric field in the transport direction is fixed to a low value (1kV/cm in this work). Second, multiple cross sections of the device are simulated using the coupled 3D Poisson and 2D Schrödinger solver (Fig. 1) integrated in the TCAD simulator GARAND from Synopsys [8]. Third, the potential and the corresponding eigenfunctions of the subbands are included in the particular scattering rates, whose expressions have been

directly developed from Fermi's Golden Rule accounting for the multi-subband quantization. These scattering mechanisms control the average electron velocity and redistribute the electron concentrations between different subbands making the calculation of any macroparameters possible, in order to characterize the system. The total energy (E_l) of a (l, k_x) state is calculated as the sum of the kinetic energy $E_{Kin} = \frac{\hbar^2 k_x^2}{2m}$ and the energy level of the subband l ($E_{subband}(l)$) in which it is located. In this work, we have included:

- (i) Acoustic Phonon Scattering: This model makes use of the short wave vector limit, in which energy is proportional to the averaged sound velocity \bar{v} . In addition, it has been characterized considering that first, it is elastic, which means that the total energy of the initial (l, k_x) and the final (l', k'_x) states must be the same ($E_l = E_{l'}$); and second, only intra-valley transitions are allowed.
- (ii) Optical Phonon Scattering: In these transitions, the initial and final states can be located in different valleys and the involved phonons have a high momentum. Accordingly, this scattering model can be handled as the intra-valley acoustic one keeping in mind that the deformation potential and the involved phonon energy must be independent of \vec{q} due to the short wave vector limit. Moreover, this mechanism is inelastic and so the final energy must satisfy $E_{l'} = E_l \pm \hbar\omega$ by absorbing or emitting a phonon. We have focused on Si NWTs in this work. The two different inter-valley transitions among the six equivalent X minima of silicon must be considered: g-type and f-type processes whose transitions are made along the same line but opposite directions and happen between ∇ valleys along different directions, respectively. We have fixed the parameters for the different branches. In particular, the set of X valleys is characterized by two-fold degeneracies. For instance, if the X1 valley is considered as the initial one, the g-type transitions set the X1 as the final valley and so it has to be treated here as an intra-valley process. On the other hand, the final valleys for f-type transitions in this example could be either X3 or X5.
- (iii) Ionized Impurity Scattering: It is relevant for all types of doped nanostructures due to the short range Coulomb interaction with the carriers. This mechanism only allows elastic and intra-valley transitions, and considers a fixed uniform ionized impurity concentration. Fermi integrals are used to compute the charge density and the Debye Length. In this work, the former parameters have been re-calculated for each bias point including the effect of the new subbands and the quasi Fermi level.

Then, the mobilities are calculated by means of the Kubo-Greenwood formula to the relaxation times of a 1D electron gas corresponding to obtain the linearized BTE. In this approach, the quasi Fermi level, which is needed in the Kubo-Greenwood formula, is determined from the carrier concentration obtained from the 3D Poisson-2D Schrödinger solver. Finally, Matthiessen rule is used to simulate the combined

effect of the scattering probabilities. Both the individual and the total mobilities of the simulated devices are reported. An important property of this semiclassical approach is the decomposition principle which, in turn, results in a feasible numerical procedure and so reduces the total computational time: the effects of different mechanisms can be independently modeled and then combined by the Matthiessen rule into a final mobility.

III. RESULTS AND DISCUSSION

The simulated device is a silicon gate-all-around (GAA) nanowire transistor (NWT). The nanowire thickness (T) and width (W) range from T=W=3nm to T=W=8nm for square and circular cross-sectional shapes. All other technological parameters remain identical: the transport orientation is [100], the gate oxide with equivalent oxide thickness (EOT) is 0.8nm, and the metal gate work function is set to 4.35eV. The gate bias is adjusted to obtain the sheet density reported in the following results. Fig. 2 shows the energy levels for a square NWT with the lowest dimension herein considered (3nm) and the largest one (8nm). The variation of the NWT width and thickness includes a valley splitting energy leaving less final states for scattering. Table I shows the effective masses corresponding to this [100] orientation, where x is the transport direction. The effective masses increase due to the quantum confinement effects. However, we use bulk effective mass values, as this work focuses on the impact of transport confinement effects on the device performance.

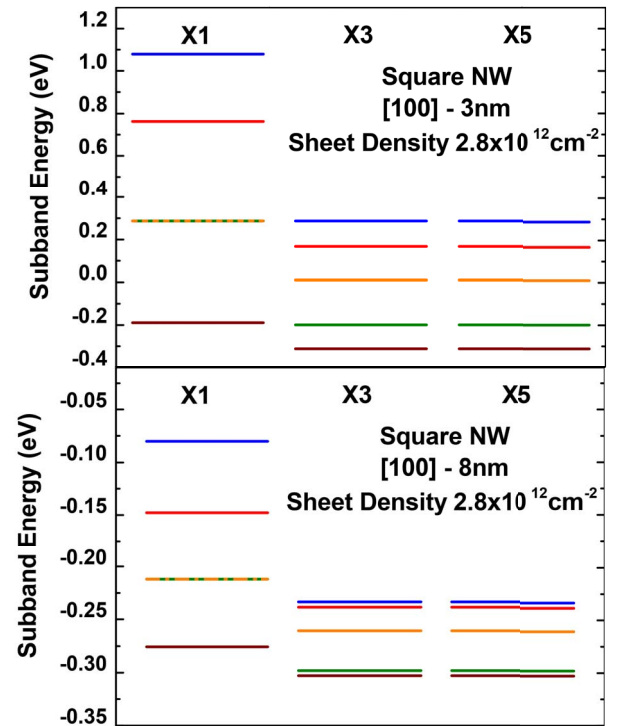


Fig. 2. Energy levels for a square NWT with 3nm (top) and 8nm (bottom) width for [100] orientation and sheet density of $2.8 \times 10^{12} \text{ cm}^{-2}$, showing band splitting for the set of valleys X1, X3 and X5.

Valley	m_x	m_y	m_z
X1	$m_l = 0.916m_0$	$m_t = 0.198m_0$	$m_t = 0.198m_0$
X3	$m_t = 0.198m_0$	$m_l = 0.916m_0$	$m_t = 0.198m_0$
X5	$m_t = 0.198m_0$	$m_t = 0.198m_0$	$m_l = 0.916m_0$

TABLE I

TRANSPORT (m_x) AND CONFINEMENT (m_y, m_z) EFFECTIVE MASSES IN THE [100] SILICON DEVICES FOR THE SET OF VALLEYS X1, X3 AND X5.

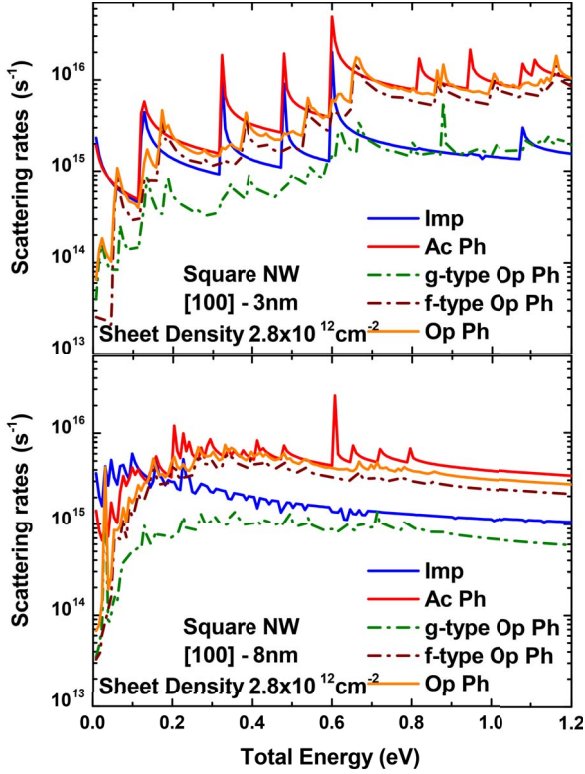


Fig. 3. Impurity scattering rate (Imp) as well as acoustic (Ac Ph), optical (including g-type, f-type and total (Op Ph)) phonon scattering rates as a function of the total energy for a square NWT with 3nm (top) and 8nm (bottom) widths for a [100] orientation and sheet density of $2.8 \times 10^{12} \text{ cm}^{-2}$.

Fig. 3 presents the scattering rates as a function of the total energy for electrons calculated for impurity, acoustic phonon, and optical phonon (including f-, g-type and total) scattering for a square NWT with 3nm (top) and 8nm (bottom) widths including 20 subbands. The multisubband effects in the scattering rates are generally more pronounced for smaller nanowire width. This is associated with the higher energy difference between the lower and upper subbands (Fig. 2), which minimizes the possible electron transitions between the subbands. It is important to highlight here that the overlap factor increases as the width decreases because it is inversely proportional to the NWT cross-sectional area. This results

in a reduction of the mobility (both taking into account the individual scattering mechanisms and the total) for highly confined NWTs (Fig. 4). Moreover, for such devices and assuming a rather large impurity concentration, the mobility is limited by both acoustic phonon and ionized impurity scattering due to their high scattering rates, especially at low energy as shown in Fig. 4.

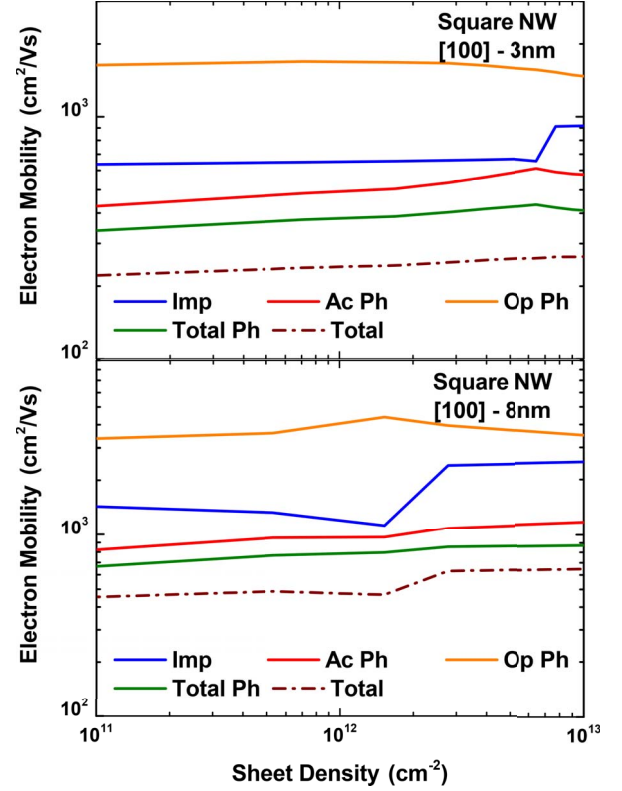


Fig. 4. Electron mobility as a function of the sheet density considering the impurity (Imp) as well as the acoustic (Ac Ph), optical (Op Ph), and total (Total Ph) phonon scattering separately as well as all combined scattering mechanisms for a square NWT with 3nm (top) and 8nm (bottom) widths for [100] orientation.

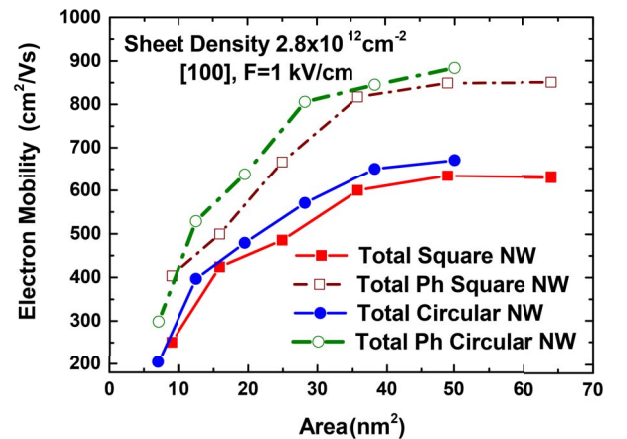


Fig. 5. Electron Mobility as a function of the area considering the impact of phonon (Total Ph) as well as both phonon and impurity scattering (Total) for a square and circular NWT with a sheet density of $2.8 \times 10^{12} \text{ cm}^{-2}$.

Finally, Fig. 5 shows the electron mobility considering only the impact of phonon scattering as well as total scattering (including both phonon and impurity) for a square and circular NWTs as a function of the cross-section area. The latter affects directly the subband energy levels and the eigenfunctions, as illustrated in Fig. 6 which shows the wavefunction modulus of the first and second subbands (X3 valleys) for 3nm and 8nm dimensions for both square and circular NWTs shape. Consequently, the direct impact associated with the change of these parameters modifies the overlap factor and so it may enhance or degrade the mobility substantially. Moreover, the results presented in Fig. 5 are in good agreement with our previous work [9], where we observed higher mobile charge in the circular NWT in comparison to the square device. As expected, the ionized impurity scattering mechanism is the dominant one for such large impurity concentration $n_0 = 10^{19} \text{cm}^{-3}$ [10].

IV. CONCLUSIONS

This work presents the implementation of the Kubo-Greenwood theory including acoustic phonon, optical phonon, and impurity scattering mechanisms for the calculation of the mobility in Si nanowire transistors. In addition, the shape and dimension of the NWTs have been also modified. The total mobility is calculated by means of the Matthiessen rule as a function of the individual scattering mechanisms. This 1D simulation module is coupled with a commercial 3D Poisson-2D Schrödinger solver in order to pre-calculate the potential profile and the eigenvalues in the NWTs. We have shown that the mobility decreases for smaller nanowire dimension NWTs due to higher multisubband effects in the scattering mechanisms. For these particular devices and assuming a rather large impurity concentration, acoustic phonon and ionized impurity scatterings insert the highest impact by controlling the total mobility due to their higher scattering rates. Moreover, we have demonstrated that the NWT shape has a strong impact on the potential profile and the corresponding eigenvalues and eigenfunctions. In conclusion, the circular NWT is a better candidate for smaller devices in terms of mobility performance.

V. ACKNOWLEDGMENT

The research leading to these results has received funding from the European Union's Horizon 2020 research and innovation programme under grant agreement No 688101 SUPERAID7. The authors would like to thank Dr. Ewan Towie for useful discussions.

REFERENCES

- [1] B. Yu, H. Wang, C. Yang, P. Asbeck, and Y. Taur, "Scaling of nanowire transistors," *IEEE Transactions on Electron Devices*, vol. 55, no. 11, pp. 2846 – 2858, 2008.
- [2] I. M. Tienda-Luna, F. G. Ruiz, A. Godoy, B. Biel, and F. Gámiz, "Surface roughness scattering model for arbitrarily oriented silicon nanowires," *Journal of Applied Physics*, vol. 110, no. 8, p. 084514, 2011.
- [3] L. S. D. Esseni, P. Palestri, *Nanoscale MOS Transistors: Semi-classical Transport And Applications*. New York, USA: Cambridge University Press, 2011.
- [4] D. Ferry and C. Jacoboni, *Quantum transport in semiconductors*. Berlin, Germany: Springer Science & Business Media, 1992.
- [5] S. Jin, T.-W. Tang, and M. V. Fischetti, "Simulation of silicon nanowire transistors using Boltzmann transport equation under relaxation time approximation," *IEEE Transactions on Electron Devices*, vol. 55, no. 3, pp. 727–736, 2008.
- [6] S. Jin, M. V. Fischetti, and T.-W. Tang, "Modeling of electron mobility in gated silicon nanowires at room temperature: Surface roughness scattering, dielectric screening, and band nonparabolicity," *Journal of Applied Physics*, vol. 102, no. 8, p. 083715, 2007.
- [7] D. Esseni and F. Driussi, "A quantitative error analysis of the mobility extraction according to the Matthiessen rule in advanced MOS transistors," *IEEE Transactions on Electron Devices*, vol. 58, no. 8, pp. 2415–2422, 2011.
- [8] Garand User Guide, <https://solvnet.synopsys.com>, Synopsys, inc., 2017.
- [9] Y. Wang, T. Al-Ameri, X. Wang, V. P. Georgiev, E. Towie, S. M. Amoroso, A. R. Brown, B. Cheng, D. Reid, C. Riddet, L. Shifren, S. Sinha, G. Yeric, R. Aitken, X. Liu, J. Kang, and A. Asenov, "Simulation study of the impact of quantum confinement on the electrostatically driven performance of n-type nanowire transistors," *IEEE Transactions on Electron Devices*, vol. 62, no. 10, pp. 3229–3236, 2015.
- [10] N. Neophytou and H. Kosina, "Atomistic simulations of low-field mobility in Si nanowires: Influence of confinement and orientation," *Physical Review B*, vol. 84, pp. 085 313 – 085 328.

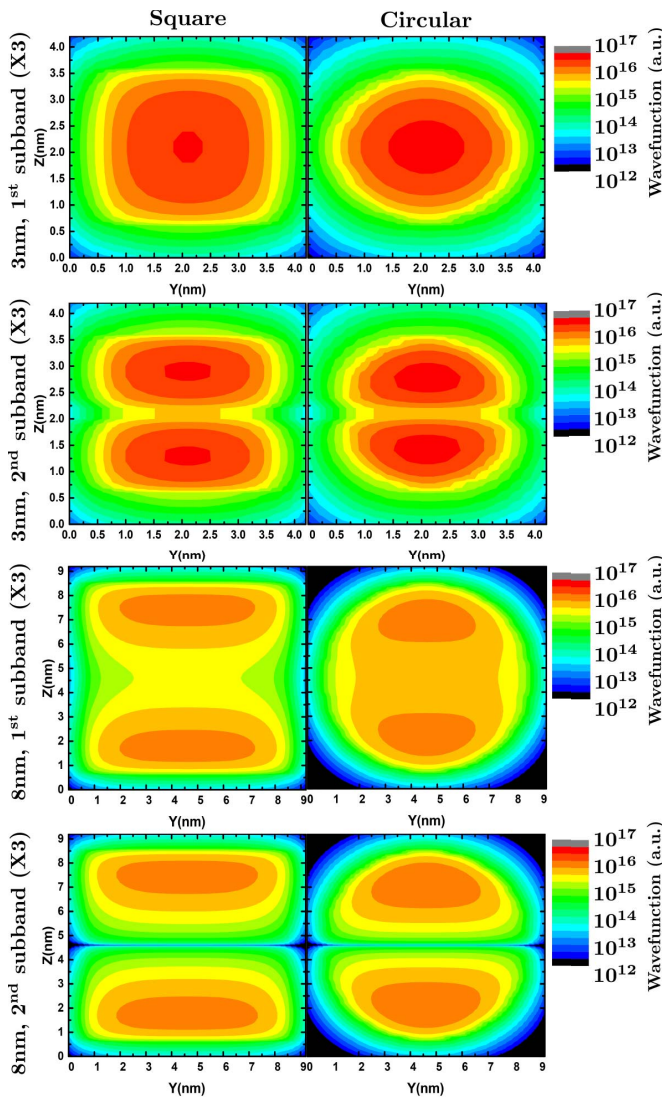


Fig. 6. Wavefunction modulus of the first and second subbands (X3 valleys) for the 3nm and 8nm diameters for both square and circular NWT shape with sheet density of $2.8 \times 10^{12} \text{cm}^{-2}$.